

## A SIMPLE PRE-OPERATIONAL MODEL FOR THE PORTUGUESE COAST

Guillaume Riflet<sup>1\*</sup>, Paulo C. Leitão<sup>2</sup>, Rodrigo Fernandes<sup>1</sup> and Ramiro Neves<sup>1</sup>

1: MARETEC DEMecanica  
Instituto Superior Técnico  
Universidade Técnica de Lisboa  
1049-001 Lisboa

e-mail: guillaume.maretec,rodrigo.maretec,ramiro.neves@ist.utl.pt, web:  
<http://www.mohid.com>

2: Hidromod Lda.  
Av. Manuel da Maia, nº 36, 3º esq.  
1000-201 Lisboa

e-mail: paulo.chambel@hidromod.pt web: <http://www.hidromod.pt>

**Keywords:** operational oceanography, downscaling, West Iberia

**Abstract.** *A three-level nested, pre-operational model of the portuguese coastal circulation is implemented with MOHID[1]. The Mercator large-scale operational North-Atlantic ocean model[2] provides initial and one-way open boundary conditions, while the MM5 mesoscale regional atmospheric forecasting model, forced by ECMRWF data, provides surface forcing. Tide is forced by the FES2004[3] tidal atlas. The open boundary conditions are based in the Flather[4] radiation scheme (sea surface height and barotropic velocity) and in a Flow Relaxation Scheme[5] (velocity, temperature and salinity). The spin up of the model is done connecting gradually the forcing terms. The results show, on a weekly-basis, a gain in spatial variability at the finer scale. Wind driven currents elaborate over the Mercator solution, providing finer scale realistic results at the surface when compared with clear sky remote-sensing SST imagery, showing fronts formation, cold finger-like structures and upwelled jets, while characteristic low frequency features such as the MW veins and the poleward slope-current[1] are evidenced within little more than a week spin-up. Other features such as transient meddies [1, 2] are also evidenced. Some forecasts results are published weekly on a Live Access Server and are also available over OpenDAP. This operational system rises as a potential tool for predicting the fate of tracers near the Portuguese coast and for providing realistic forcing for local coastal models applied to estuaries or hydrographic basins or other client applications such as the Oil observer, also presented in this work*

## 1 INTRODUCTION

A three-level nested tridimensional hydrodynamic model was applied for the west Iberia coast and refined near the Estremadura promontory using MOHID. Realistic forcing was used provided by the large-scale North-Atlantic Mercator-Océan[2] oceanic solution and by the atmospheric MM5 model run at meteo-IST[6]. Tide is forced using the FES2004 solution[3]. The Psy2v2R1 Mercator-Océan solution consists of a weekly 14 day forecast and a last 7 day reanalysis. The meteo-IST solution consists in a 7 day atmospheric forecast. A pre-operational system was mounted at Maretec-IST that pre-processes the forcing solutions, runs the hydrodynamical model and serves every monday nowcasts and forecasts until thursday of the general circulation off west Iberia. The results are stored in netcdf files and served by a LAS and an Opendap[7] server.

While the work of Coelho [1] focused more on the study of the upwelling process, the poleward current and the Portugal Current system, the current work aims at investigating the model's capability of reproducing accurately the known processes near the Gulf of Cádiz up to the Estremadura promontory in forecast mode. Namely the Mediterranean outflow spreading pathway and the ENACW entrainment near the gulf of Cádiz. To do so, results from the model starting in mid-November 2006 up to mid-February 2007 were analysed.

## 2 DOWNSCALLING

The MOHID hydrodynamical numerical model solves the Navier-Stokes equations of a rotating fluid in a  $\beta$  plane. The geophysical fluid is constrained to the hydrostatic and the Boussinesq approximations, as a practical result of a dimensional analysis[8].

The numerical solver uses a finite-volumes approach[9] similar to the one described by Chu[10].

MOHID solves also a seawater density non-linear state equation depending on pressure, salinity and potential temperature originally proposed by Millero[11].

Finally, to calculate the turbulent vertical mixing coefficient, MOHID embeds GOTM[12][13].

The mixing-length scale parametrization proposed by Canuto[14] is used.

The horizontal discretization is an Arakawa C grid[16]. The vertical coordinate is hybrid and generic, allowing to choose between z-level, sigma and lagrangian coordinates[17].

The baroclinic pressure gradient term is always calculated using a z-level approach, with a linear interpolation, in order to minimize spurious pressure-gradient errors that induce unrealistic vertical velocities[18] [19][20].

In this application, the 2D model uses a sigma coordinate, and the tridimensional models use a lagrangian vertical coordinate with shaved-cells at the bottom[21] and a z-level initial condition.

The temporal numerical scheme is an alternate direction semi-implicit (ADI) method[22].

The spatial discretization numerical scheme is a total variation diminishing (TVD) scheme[23].

The modelled domains description and configuration follows in the next subsections. Ta-

<b>Boundary conditions</b>	
<b>Surface</b>	<b>models</b>
Wind stress forcing from MM5 winds through equation 1.	P, C
Interpolated heat fluxes from MM5 data.	<i>P</i> and <i>C</i>
<b>Open Boundary Conditions</b>	<b>models</b>
<i>FRS</i> [5] of the <i>M-O</i> solution for U, V, T and S.	<i>P</i> and <i>C</i>
Interpolation of $\eta$ , U, V, T and S from <i>M-O</i> .	<i>P</i> and <i>C</i>
Barotropic mode <i>Blumberg</i> radiation[24].	<i>WI</i>
Barotropic mode <i>Flather</i> radiation[4].	<i>P</i> and <i>C</i>
Sponge layer.	<i>P</i> and <i>C</i>
<b>Land boundary</b>	<b>models</b>
Freshwater discharges.	<i>P</i> and <i>C</i>
Null fluxes of (U,V).	<i>WI</i> , <i>P</i> and <i>C</i>
<b>Bottom boundary</b>	<b>models</b>
Bottom stress forcing according to equation 8.	<i>WI</i> , <i>P</i> and <i>C</i>

Table 1: Nested models boundary conditions. The abbreviations definitions are: Zonal and meridional velocity components ( $U$ ,  $V$ ), potential temperature ( $T$ ) and salinity ( $S$ ), water level relative to a reference level ( $\eta$ ), flow relaxation scheme (*FRS*), Mercator-Océan solution(*M-O*), western Iberia barotropic model (*WI*), portuguese Iberian coastal model(*P*), Estremadura promontory model (*C*).

bles 1 and 2 summarize the initial conditions and the boundary conditions.

In order to obtain coherent open boundary conditions (OBC), a good reference solution is mandatory[26]. The high resolution solution of the Northern Atlantic and the Mediterranean basin provided by Mercator-Océan, **PSY2v2r1**, is likely to be a reliable solution available[2][27] that reproduces realistically the Northern Atlantic circulation and in particular the western Iberian coastal circulation and the Gulf of Cadiz circulation. While assimilating *in-situ* data, remote sensed sea level anomaly (SLA) and sea surface temperature (SST), as well as atmospheric forecasts fed by the European Centre for Medium Range Weather Forecast (ECMWF), the Mercator solution reproduces accurately the main characteristics of the circulation off western Iberia peninsula. Namely, it reproduces the Mediterranean Outflow (MO), several downstream Mediterranean veins[28][29][30] and also the formation of meddies near Cape St.Vincent and over the Estremadura bank[31][29]. However, the number of meddies formed by the model at St.Vincent Cape is inferior relatively to the observations. According to Drillet[2], this is probably due to the z-level vertical coordinate choice. Indeed, such a choice of coordinates is seemed to underestimate the dense water sinking downstream of the Gibraltar strait because of the intense nature of the MO near the Gibraltar strait. This problem was coped by Drillet[2] with a stronger relaxation towards Reynaud’s[32] climatology downstream of the Gibraltar strait[2]. Unfortunately, the bias of the results in Reynaud’s

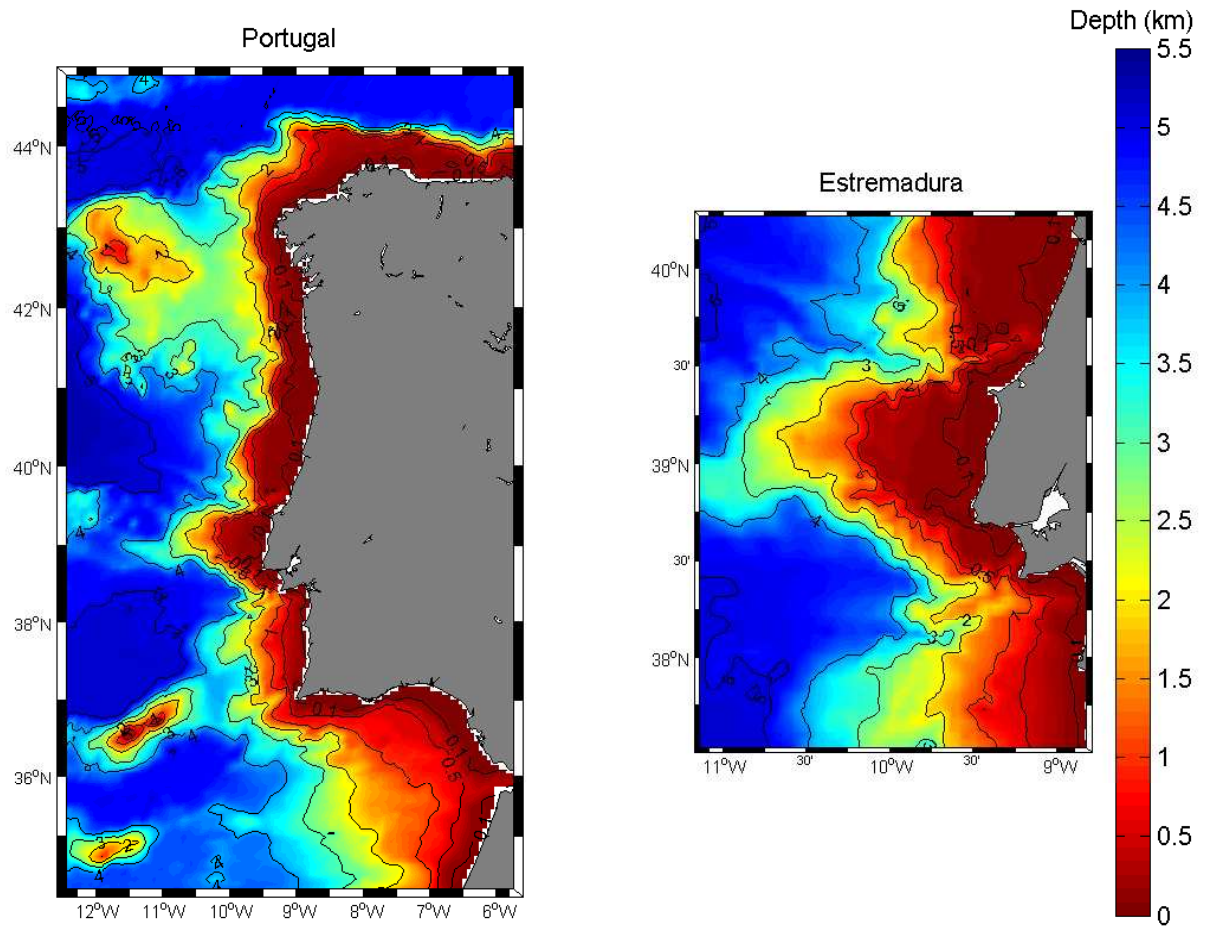


Figure 1: On the left panel, the Western Iberia coast baroclinic model bathymetry. The domain is labeled *P*. Bounded by  $[-12.6^\circ - 5.5^\circ] W \times [34.4^\circ - 45.0^\circ] N$ .  $0.06^\circ$  spatial resolution. On the right panel, Portugal continental central regional coastal model bathymetry, labeled *C*. Bounded by  $[-11.2^\circ - 8.8^\circ] W \times [40.3^\circ - 37.5^\circ] N$ .  $0.02^\circ$  spatial resolution. Baseline data from ETOPO 2'[25] on both panels.

<b>Initial conditions</b>	
U, V, S and T are interpolated from the <i>M-O</i> solution.	<i>P</i> and <i>C</i>
$\eta$ is initialized to a reference level.	<i>WI</i> , <i>P</i> and <i>C</i>
<b>Assimilation</b>	
U, V, T and S <i>FRS</i> according to equation 5.	<i>P</i> and <i>C</i>
<b>Spin up</b>	
Baroclinic force and wind forcing ignition over 10 inertial periods.	<i>P</i>
<i>FRS</i> and <i>Flather</i> radiation ignition over 10 inertial periods.	<i>P</i>

Table 2: Nested models' initial conditions, assimilations and spin-up. The abbreviations definitions are: Zonal and meridional velocity components ( $U$ ,  $V$ ), potential temperature ( $T$ ) and salinity ( $S$ ), water level relative to a reference level ( $\eta$ ), flow relaxation scheme (*FRS*), modèles de Mercator-Océan (*M-O*), western Iberia barotropic model (*WI*), portuguese Iberian coastal model(*P*), Estremadura promontory model (*C*).

climatology are propagated and an inferior temperature and salinity of about  $0.75^{\circ}C$  and  $0.15\ psu$ , respectively, is obtained[2] when compared with known measurements such as in the works of Iorga[30]. This said, Mercator's solution is likely to be a good candidate as a reference solution capable of forcing a model operationally. The Mercator solution extraction domain ranges approximately from  $24.5^{\circ}W$ ,  $28^{\circ}N$  to  $4^{\circ}W$ ,  $51^{\circ}N$ .

The Mercator solution is interpolated to the MOHID meshes in two steps:

1. An interpolation using a triangulation method is used for each bidimensional layer. It produces an auxiliary field with the same horizontal mesh than the MOHID model.
2. A linear interpolation of each vertical column of the auxiliary field to the MOHID columns is applied. This step will produce a field consistent with the MOHID mesh.

The Mercator solution is labeled herein *M-O*.

The model is coupled with MM5 [33] atmospheric model from IST in *offline* mode. The three-level nested atmospheric model is forced with the Global Forecasting System (GFS)7 day forecast over the region bounded by  $20^{\circ}W$ ,  $28^{\circ}N$  and  $5^{\circ}W$ ,  $50^{\circ}N$ . The nested models resolution are 81, 27 and 9 km and are composed of 25 vertical layers. It simulates winds, sensible heat, latent heat, solar radiation, precipitation, evaporation, specific humidity, cloud cover and atmospheric pressure.

The Finite Element Solutions (FES) are tidal atlases released nearly every two years, being the latest one of them the FES2004[3]. These tidal atlases result from model computation in unstructured meshes with spectral element methods(CEFMO and MOG2D-G code) applied to the nearly-linearized shallow water equations. The FES model assimilates remote-sensing data (Topex/Poseidon, ERS1 and ERS2 satellite altimetric data

assimilated with the CADOR code), in-situ tidal gauges measurements, and tide atmospheric forcing (ECMWF). Being a state-of-the-art atlas, it is recommended for tidal applications[3].

The surface fluxes of the MOHID models are composed of momentum (induced by wind stress and calculated by a diffusive term), sensible heat, latent heat, evaporation, precipitation and infrared radiation. The latter term is the system's response to the solar radiative forcing discussed further below.

Wind forcing is calculated[34] according to equation 1

$$\tau_w^u = \rho_a C_a u_{10} \sqrt{u_{10}^2 + v_{10}^2} \quad (1)$$

where  $\tau_w^u$  is the surface stress induced by wind,  $\rho_a = 1.25 \text{ kg/m}^3$  is air density,  $C_a$  is a drag coefficient whose range is described in Leitao2003[35], finally  $u_{10}$  and  $v_{10}$  are the horizontal components of air speed at 10 m of height above the sea surface.

The solar radiation term is decomposed into the long wave and short wave penetration into the water column. It's physically modelled by a penetrating heat source term at the surface and decaying along the water column. The decay constants are two-fold and depend on the type of waters and the type of wave-lengths. The system's physical response to this radiative forcing is the infrared radiation, modelled as an outwards surface flux.

Two methods of open boundary conditions (OBC) are frequently used: radiative methods, based on the Sommerfeld condition,

$$\frac{\partial \Phi}{\partial t} + \vec{c} \cdot \vec{n} \Phi = 0 \quad (2)$$

and nudging (or relaxation) methods. For an interesting review on the main OBC methods see Blayo[26].

According to his work, the Flather radiation method[4], consisting of the Sommerfeld condition combined with the continuity equation, is best for radiating the water level. However, it requires an external water level and an external barotropic flux to be known in order to be used. Indeed the Flather radiation method may be equated at the model's open boundaries in the following way:

$$(\vec{q} - \vec{q}_{ref}) \cdot \vec{n} = (\eta - \eta_{ref}) (\vec{c} \cdot \vec{n}). \quad (3)$$

where  $\vec{q}$  and  $\vec{q}_{ref}$  are the model's and the external solution's barotropic flux, respectively;  $\vec{n}$  is the external open boundary normal vector;  $\eta$  and  $\eta_{ref}$  are the model's and the external solution's water level.  $\vec{c}$  is the surface gravity wave's celerity, approximated by  $\sqrt{gH} \vec{r}$ , where  $\vec{r}$  is the propagation direction unit vector.

When only the external water level is known, then the Blumberg method[24], consisting of a combination between a nudging term and the Sommerfeld condition, may be used as an alternative:

$$\frac{\partial \eta}{\partial t} + \vec{c} \cdot \vec{n} \nabla \eta = -\frac{\eta - \eta_{ref}}{T_{lag}} \quad (4)$$

$\eta$  is the water level,  $\eta_{ref}$  is the reference water level,  $\vec{c}$  is the external wave celerity,  $\|\vec{c}\|$  is estimated to be  $\sqrt{gH}$ ,  $\vec{n}$  is open boundary external normal vector,  $g$  is the local gravity acceleration,  $H$  is the depth and  $T_{lag}$  is the relaxation decay time. The Blumberg method relaxation decay time ranges from a shorter 200 s in deep waters to a longer 2000 s in coastal shallow waters.

For the other variables, where no accurate estimation of their celerity is available, another class of OBC method is used: the relaxation method. It consists on a looser approach to the clamped (Dirichelet) conditions on the open boundary  $\Gamma$  of the domain  $\Omega$ [26], where a relaxation decay time is introduced and an additional domain is created  $\Omega_s$ , 10 cells wide, which interfaces between  $\partial\Omega \equiv \Omega \cap \Omega_s$  and  $\Gamma$ . This approach is commonly regarded as a Flow Relaxation Scheme (FRS)[5]. The relaxation term writes

$$\frac{\partial \Phi}{\partial t} = -\frac{\Phi - \Phi_{ref}}{\tau} \quad (5)$$

where  $\Phi$  is the relaxed variable,  $\Phi_{ref}$  is the reference solution and  $\tau$  relaxation time decay constant. The time decay varies from  $3 \times 10^4$  s on  $\Gamma$  to  $1 \times 10^9$  s on  $\partial\Omega$ , 10 cells to the interior. Thus the computed domain becomes  $\Omega \cup \Omega_s$ . Following Martinsen and Engedahl[5], the FRS approach is used as the main downscaling technique for  $S$ ,  $T$ ,  $u$  and  $v$ , respectively the salinity, the potential temperature, the zonal velocity component, and the meridional velocity component.

Additionally, in order to smooth out the nudging at  $\Omega_s$ , a sponge layer, consisting of a high viscosity layer, is implemented. The viscosity terms range, inside  $\Omega_s$ , from  $1.8 \times 10^4$   $m^2/s$  at  $\Gamma$  to  $10$   $m^2/s$  on  $\partial\Omega$ . In  $\Omega$ , the horizontal viscosity is considered constant at  $10$   $m^2/s$ . Finally, in order to filter out the high frequency noise generated by resonant open boundary spurious reflections, a laplacian biharmonic filter is implemented in the primitive equations. Typical values of the biharmonic filter coefficient may vary between  $1 \times 10^{10}$   $m^4/s$  and  $1 \times 10^9$   $m^4/s$ .

A null mass and momentum flux is imposed at the lateral land boundary:

$$\vec{v} \cdot \vec{n} = 0 \quad (6)$$

where  $\vec{v}$  is the velocity vector and  $\vec{n}$  is the normal vector at the land-water interface. A freshwater discharge with daily values is imposed near the Tagus area for both models. The data source comes from the publicly available *INAG* (*Instituto da Água*) web-site<sup>1</sup>

---

<sup>1</sup><http://snirh.pt/>

and, in this application, spans the 2004-2006 period. The 2006 year is replicated and used in 2007 simulations as an estimative of realistic daily freshwater discharges.

The bottom stress is given by [34]

$$\tau_b^u = \rho_0 C_D u_b \sqrt{u_b^2 + v_b^2} \quad (7)$$

where  $\tau_b^u$  is the bottom stress,  $u_b$  and  $v_b$  are the near-bottom velocity horizontal components,  $\rho_0$  is the reference density. The drag coefficient is given by[35],

$$C_D = k / \ln \left( \frac{z_D + z_0}{z_0} \right)^2 \quad (8)$$

where  $z_D$  is the bottom height and  $z_0$  is the roughness length. The Von Karman constant is set to[35]  $k = 0.4$ . The bottom roughness length is set to  $z_0 = 0.0025 \text{ m}$  for all models.

## 2.1 Barotropic model *WI*

Since the Mercator solution is rigid-lid and doesn't takes into account the tide effect correctly, the idea came that a tidal reference solution should be built and linearly superposed to the Mercator reference solution in order to force coastal models with oceanic and tidal effects. Thus, a barotropic model model of western Iberia was created named *WI*, forced only with the FES2004 tidal atlas solution. The atmospheric forcing from the MM5 model was not be included, but the S1 and S2 components of the FES2004 solution already take into account the atmospheric tide forcing[3]. The bathymetry baseline data is taken from the ETOPO 2'[25]. The domain has  $0.06^\circ$  horizontal and  $180 \text{ s}$  temporal resolution and is bounded within the interval  $[-13.7^\circ - 5.3^\circ] \text{ W} \times [33.5^\circ 46.1^\circ] \text{ N}$ . The water level reference solution is computed from the FES2004 tidal harmonic components. The Blumberg radiative condition[24](eq. 4) is applied at the open boundaries. A biharmonic filter is implemented in the domain to filter out high-frequency noise and has a  $10^9 \text{ m}^4/\text{s}$  coefficient. The barotropic force is gradually connected over 10 inertia periods.

## 2.2 Portuguese coastal model *P*

A tridimensional baroclinic model is nested to the latter. It may be viewed as the enhanced version relative to Coelho [1]. Composed by 42 vertical layers, it possesses a  $0.06^\circ$  horizontal resolution and a  $180 \text{ s}$  temporal resolution (Coelho only had 18 layers and  $8.5 \text{ km}$  of resolution). Bounded by  $[-12.6^\circ - 5.5^\circ] \text{ W} \times [34.4^\circ 45.0^\circ] \text{ N}$  the model's forced with the MM5 atmospheric forcing reference solution at the surface, and by the barotropic model *WI* and the Mercator model reference solutions *M-O* at the open boundaries. The atmospheric forcing is slowly started over 10 inertia periods. The level is radiated by a Flather radiation method[4] whose barotropic flux and level reference solution,  $q_{ref}$  and  $\eta_{ref}$ , are given by the linear superposition of the barotropic fluxes and water levels of *WI* and *M-O* respectively,  $q_{ref} = q_{WI} + q_{M-O}$  and  $\eta_{ref} = \eta_{WI} + \eta_{M-O}$ . Also, the Flather radiation method is slowly activated over 10 inertia periods. Furthermore, a FRS[5] is

applied to  $S$ ,  $T$ ,  $u$  and  $v$ . The baroclinic force is slowly activated over 10 inertia periods. The biharmonic filter coefficient is set to  $1 \times 10^{10} \text{ m}^4/\text{s}$ . Turbulent horizontal viscosity is estimated roughly to  $10 \text{ m}^2/\text{s}$  inside the domain, but a sponge layer is applied at the open boundaries, ten cells wide. The sponge layer evolves gradually from a viscosity of  $10^2 \text{ m}^2/\text{s}$  inside of the domain, up to  $1.8 \times 10^4 \text{ m}^2/\text{s}$  at the boundary. The modelled domain is labeled  $P$  and its bathymetry is shown in figure 1.

### 2.3 Estremadura model $E$

The Estremadura bank regional model, bounded by  $[-11.2^\circ - 8.8^\circ] W \times [40.3^\circ 37.5^\circ] N$ , differs from  $P$  in the horizontal spatial resolution and in the temporal resolution, respectively of  $0.02^\circ$  and  $90 \text{ s}$ . It also differs from  $P$  in the Flather radiation (eq. 3) where the reference level and the barotropic flux come only from the  $P$  model. This model should be able to reproduce the evolution of finer-scale physical processes. In particular those associated to the Rossby baroclinic radius of deformation who, near the western Iberia zone, should have approximately a  $25 \text{ km}$  radius [36]. Stevens[37] suggests that a resolution ten times higher than the first baroclinic Rossby radius of deformation (i.e. circa  $2.5 \text{ km}$ ) is required in order to resolve the associated finer scale physical processes. In the western Iberia region,  $0.06^\circ$  of horizontal resolution doesn't meets the latter requirement but  $0.02^\circ$  does. It is, thus, expectable that finer-scale processes should appear in this model. These processes are filtered out by the rougher resolution in the  $P$  model. This model is labelled  $C$  (as in Centre), and its bathymetry (interpolated from ETOPO 2'[25]) is illustrated in figure 1.

## 3 THE RESULTS

There are two modes of forcing:

- The analysis mode, where the oceanic forcing uses the analyzed  $M-O$  solution.
- The forecast mode, where the oceanic forcing uses the prediction mode  $M-O$  solution.

Either way, the atmospheric forcing always used the  $MM5-IST$  7 day forecasting solution. This provided less reliable results for the analysis mode runs. It is an issue to be addressed in the near future.

The models are scheduled to run the past 7 days in analysis mode and the next 7 days in forecasting mode. The 14 day run requires 48 hours to finish, thus giving in the end, 5 days of ocean forecasts. The time to complete the runs can be optimized, perhaps reducing to a 40 hours run.

The first 7 days run is the model's spin-up, allowing it to slowly activate the wind-forcing, the baroclinic forces and the radiative methods while it adjusts a velocity field to the initial density field. An alternate method consisting of performing a calculus continuation from the end of the last analysis is considered. However, for initialization purposes, performing

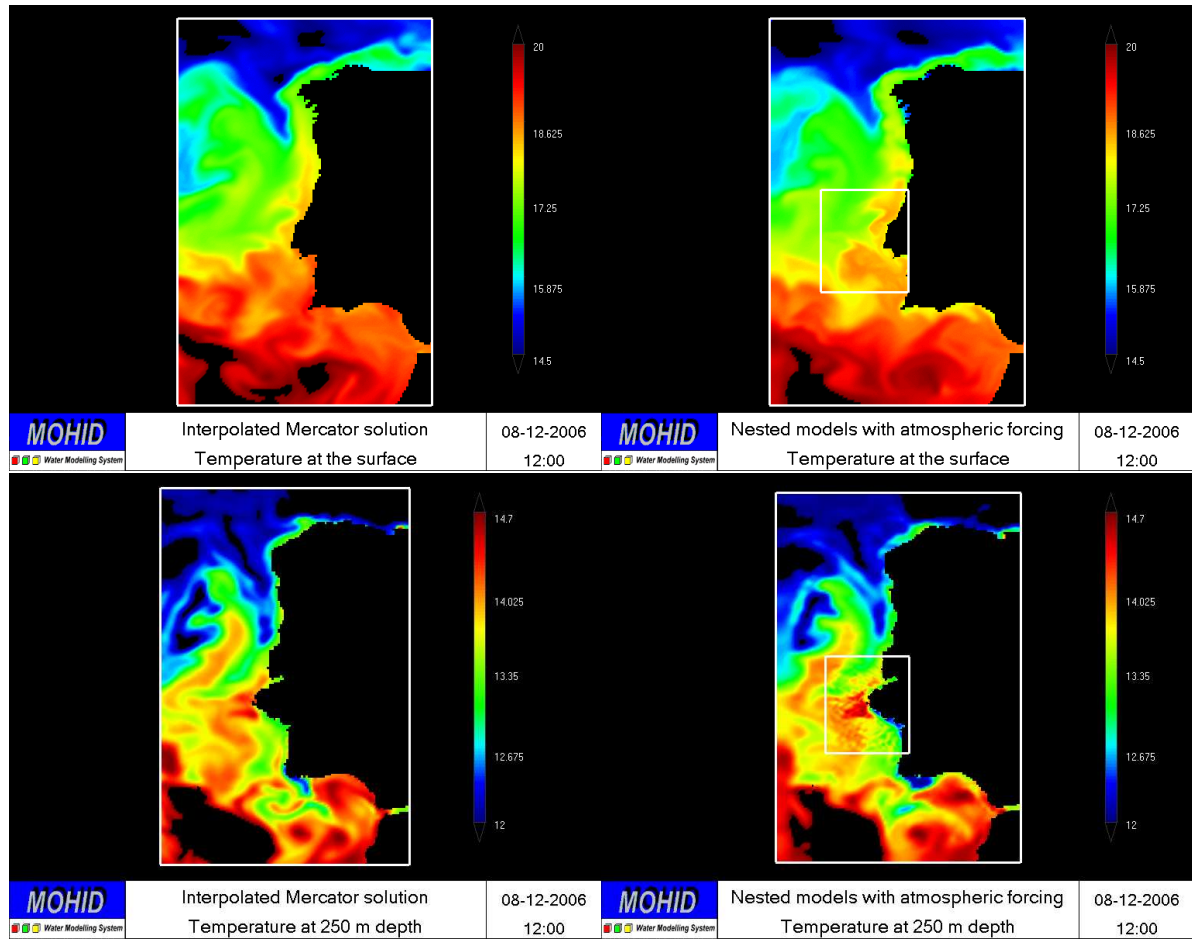


Figure 2: To the left, the interpolated temperature fields of the  $M-O$  solution. To the right, the superposition of the temperature fields of the  $C$  model over the  $P$  model. The temperature scale's interval is  $[14.5\ 20.0]^{\circ}C$  at the surface (top) and  $[12.0\ 14.7]^{\circ}C$  at 250 m (bottom). The graphical tool is Mohid GIS.

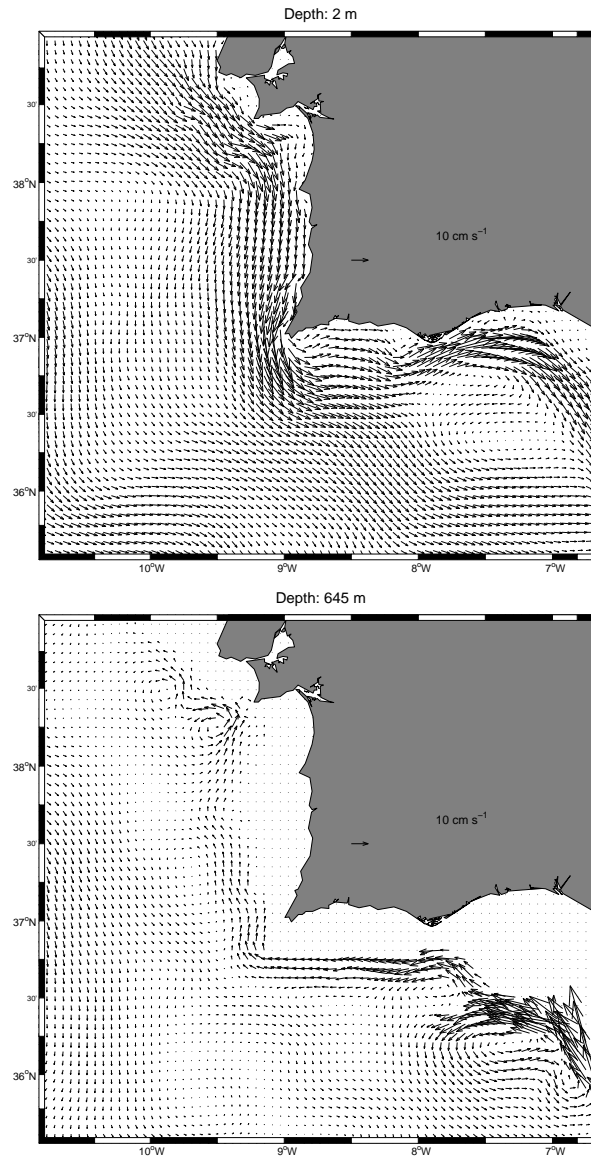


Figure 3: Horizontal distribution of velocity ensemble average at 2 m depth for the top panel and 645 m depth for the bottom panel. Two main branches of the MW spreading pathways are well pronounced in the bottom panel: the poleward slope current branch, and the cyclonic recirculation flowing southward.

a 7 day spin-up every week is thought to be numerically more robust than undertaking a hot start, since the latter method would induce a lot of high-frequency noise in the  $\eta$ ,  $u$  and  $v$  terms. Two common approaches are used to tackle inconsistent current and level initial fields: one is based in an inverse model method which consists of analyzing previously the initial fields and, by means of adequate constraints, to generate a physically consistent initial velocity and level fields. But this method is generally quite slow to implement and demands robust computerized resources (for example the VIFOP tool [38]). Another approach is to create a digital filter by means of an adequate convolution product with a high-frequency cut-off distribution [39]. A third method is to use proven consistent velocity and level fields to start with, such as the null velocity and constant reference level fields. This work undertook the latter method.

A comparison between the Mohid results and the Mercator solution is undertaken. The first increment of the comparison is the visual inspection. Results of the temperature and salinity fields of the Mercator solution can be visually inspected against results of the Mohid solution in figure 2 for a 2006 mid-December day. The  $C$  model results are superimposed over the  $P$  model results. We can observe a general gain in the spatial variability of fronts forming in the  $C$  domain, for all depths and all variables (not shown). This was expected due to the finer resolution of the  $C$  domain.

At the depth of the thermocline over the Estremadura bank, at the  $C$  domain at 250 m depth, internal waves interference patterns can be observed in figure 2 due to reflections at the domain's boundaries. These interferences occur during the model's spin-up (starting about the 3rd day) and are rapidly dissipated (by the 7th day). They appear near the thermocline depth, which is where the vertical density gradient is steeper, and which is where the number of vertical layers is higher. An alternative hypothesis is that these internal waves were produced at different generation points in the Estremadura promontory, and that their interaction yields the interference pattern. This shows that the  $C$  domain is able to generate internal waves. This type of internal wave interference pattern doesn't appear in the  $P$  domain. This is probably due to an insufficient horizontal resolution, or simply because the domain's characteristic length and time period isn't compatible with the formation of internal waves. Near the Iberian coastal area, the characteristic length of internal waves is estimated to vary between 20 – 30 km (close to the the first baroclinic Rossby radius of deformation). According to Stevens[40], a tenfold resolution is required in order to accurately reproduce frontogenesis and baroclinic instabilities, i.e. a 2km resolution in the West-Iberia coastal area. Hence, the latter argument sustains the hypothesis that the  $P$  domain has a non-permitting baroclinic instability resolution.

The work of Drillet[2] validates the capability of the Mercator solution of accurately reproducing the meddies life-cycle (since their genesis near Cape São Vicente or over the Estremadura bank to their dissolution in Atlantic waters) as well as the characteristic Mediterranean veins of the area. Nonetheless, as we initialize each time with a null velocity and level field, a 14 day run isn't sufficient for our model to generate fully developed meddies as these yield characteristic times of formation of at least 80 days[41]. Thus, by

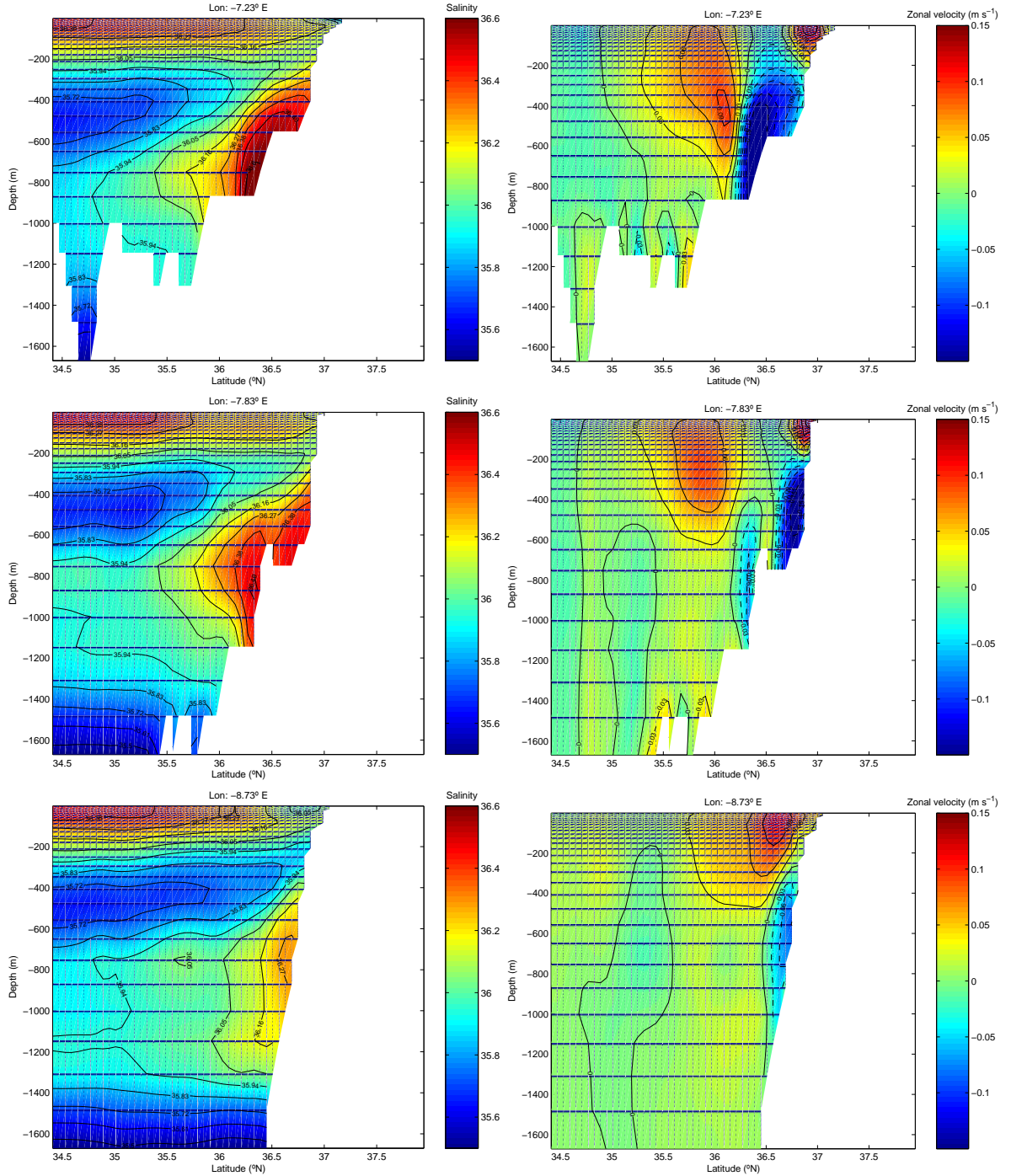


Figure 4: On the left panel, ensemble averages of salinity contours of [35.5, 35.52, 35.83, 35.94, 36.05, 36.16, 36.27, 36.38, 36.49, 36.6] and color maps in the interval [35.5 36.6]. On the right panel, ensemble averages of zonal velocity contours of [-.15, -.12, -.09, -.06, -.03, .0, .03, .06, .09, .12, .15]  $m s^{-1}$  and color maps in the interval [-.15 .15]  $m s^{-1}$ . The plots are meridional sections in the Gulf of Cádiz at longitudes 7.23°W, 7.83°W and 8.73°W from top to bottom, respectively. They show how the MO shifts from a bottom current to a buoyancy driven intermediate depth jet current.

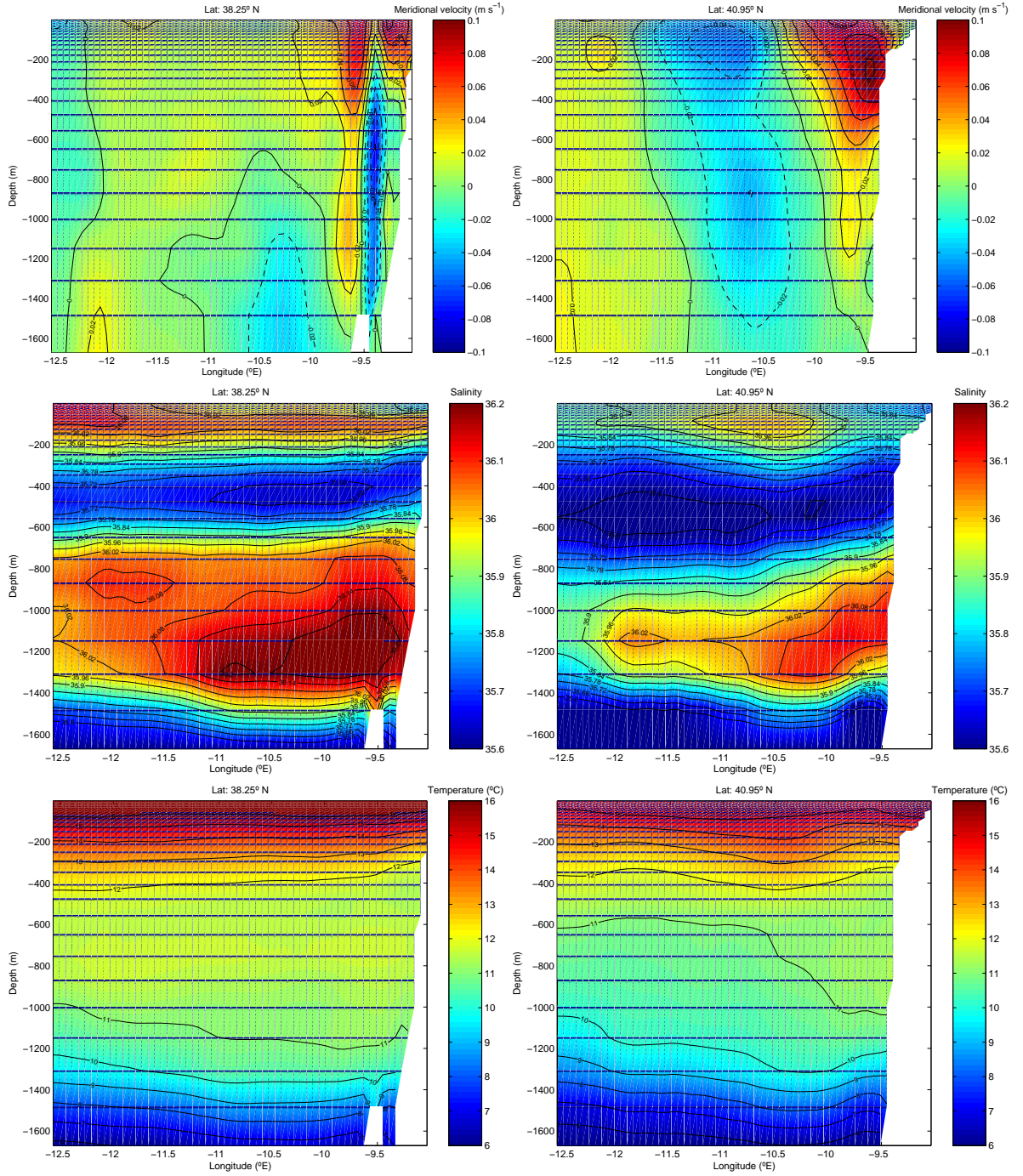


Figure 5: On the top panels, ensemble averages of meridional velocity contours of  $0.1 m s^{-1}$  apart and color maps in the interval  $[-.1.1] m s^{-1}$  are shown. Positive velocities are equatorward and negative velocities are poleward. On the middle panels, ensemble averages of salinity contours of  $[35.6, 35.66, 35.72, 35.78, 35.84, 35.90, 35.96, 36.02, 36.08, 36.14, 36.2]$  and color maps in the interval  $[35.6, 36.2]$  are shown. On the bottom panels, ensemble averages of temperature isocontours of  $1^{\circ}C$  apart and color maps in the interval  $[6, 16]^{\circ}C$  are shown. The plots are zonal sections off the Portuguese coast at latitudes  $38.25^{\circ}N$ , for the left panel; and  $40.95^{\circ}N$ , for the right panel.

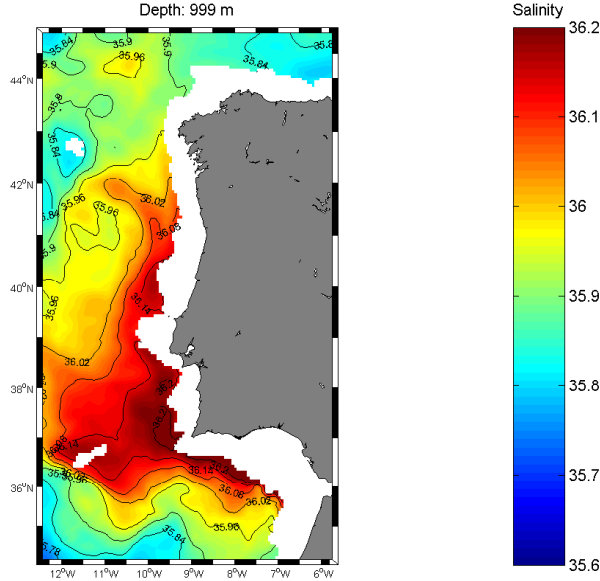


Figure 6: Color map and contours of salinity distribution ensemble average at 1000 m depth ranging in interval [35.6 36.2] showing the spreading pathway of the MO off western Iberia. Contour lines are valued [35.6, 35.78, 35.84, 35.9, 35.96, 36.02, 36.08, 36.14, 36.2].

these standards, the model is de-facto non-meddy permitting. This problem is expected to be solved with longer runs or with calculus continuation from the last analysis run. However, the salinity and temperature profiles and the qualitative aspect of the density-driven currents can be analyzed and expected to yield realistic results. Thus each 14 day run was integrated in time, and the ensemble mean of these averages spanning from mid-november 2006 to mid-february 2007 was calculated.

Given an ensemble of fields  $\{\psi^1, \psi^2, \dots, \psi^N\}$  that evolve over a period of time  $T$ , we can split their time average

$$\overline{\psi^i} \equiv \frac{\int_0^T \psi^i(t) dt}{T} \quad (9)$$

into the spin-up characteristic time  $\tau$  component,  $\psi^{i'}$ , (described in the used methodology) and the rest,  $\widehat{\psi^i}$ , i.e.

$$\overline{\psi^i} = \frac{\int_0^\tau \psi^i(t) dt}{\tau + (T - \tau)} + \frac{\int_\tau^T \psi^i(t) dt}{\tau + (T - \tau)} \equiv \frac{\overline{\psi^{i'}} \tau}{T} + \frac{\widehat{\overline{\psi^i}} (T - \tau)}{T}. \quad (10)$$

Hence their ensemble average can write

$$\langle \overline{\psi} \rangle \equiv \sum_i^N \overline{\psi^i} / N$$

$$\begin{aligned}
 &= \sum_i^N \frac{a \overline{\psi}^{i'} + b \widehat{\psi}^i}{N} \\
 &= a \langle \overline{\psi}' \rangle + b \langle \widehat{\psi} \rangle,
 \end{aligned} \tag{11}$$

where  $a = \tau/T$  and  $b = (T - \tau)/T$ . Thus, in our case, it is a reasonable assumption to state that

$$|\langle \overline{\psi}' \rangle| < |\langle \widehat{\psi} \rangle|, \tag{12}$$

as regards the  $\eta$ ,  $u$  and  $v$  fields; since all start with null values and since tide, windstress and density gradient forces are gradually connected during the spin-up period time,  $\tau$ . Hence, minding the Schwarz inequality,

$$\begin{aligned}
 |a \langle \overline{\psi}' \rangle + b \langle \widehat{\psi} \rangle| &< a |\langle \overline{\psi}' \rangle| + b |\langle \widehat{\psi} \rangle| \\
 &< a |\langle \widehat{\psi} \rangle| + b |\langle \widehat{\psi} \rangle|,
 \end{aligned} \tag{13}$$

thus, from equation 11 and since  $a + b = 1$ , the latter inequality is equivalent to

$$|\langle \overline{\psi} \rangle| < |\langle \widehat{\psi} \rangle|. \tag{14}$$

Inequality 14 has a strong physical meaning, assuming that equation 12 holds. It means that the ensemble average properties for  $\eta$ ,  $u$  and  $v$  are probably underestimated and that this should be minded when looking at  $\langle \overline{\eta} \rangle$ ,  $\langle \overline{u} \rangle$  and  $\langle \overline{v} \rangle$  results.

Figure 3 shows the ensemble average according to equation 11 of the horizontal velocity near the surface and 645 m deep. At the surface a wind-driven equatorward flow evolves whereas at the subsurface an intermediate depth MW undercurrent evolves and branches. Two main branches are depicted by the model's results: a poleward slope current branch that flows leaned against the Portuguese shelf whereas, south of the Strait of Gibraltar, another branch is formed showing a cyclonic recirculation southward that will feed the Canary currents system. This MW spreading pathways scenario is consistent with the ones evidenced in the works of Bower[29] and Iorga[30].

Figure 4 is a series of meridional cross sections of ensemble averages according to equation 11 of salinity and zonal velocity in the Gulf of Cádiz at longitudes  $7.23^\circ W$ ,  $7.83^\circ W$  and  $8.73^\circ W$ . The cross sections show the formation of deep Mediterranean Water flowing past the Gibraltar Strait into the Atlantic, forming the Mediterranean salt tongue[29]. The overflow of denser Mediterranean waters entrains at the Gibraltar Strait under the less dense North Atlantic Central Water (NACW) and downslopes[42] along the continental slope on the northern margin, south of Algarve as a density-driven current. As it flows westwards, at about  $8^\circ W$ , it reaches neutral buoyancy and detaches from the bottom

near 700 *m* depth and continues as a boundary undercurrent, then it descends down to 1000 *m* depth[29] near 8.5° *W* (fig.4) where it seems to attain hydrostatic equilibrium. The Mediterranean salt tongue turns northward past Cape São Vicente and probably continues flowing northward to as far as Porcupine bank (50° *N*)[30].

Figure 5 is a series of zonal vertical cross sections of ensemble averages of salinity, temperature and meridional velocity of western Iberia at 38.25°*N* and 40.95°*N*. Figures 4 and 5 evidence the main Mediterranean vein by the anomalous salinity maximum. The depth of salinity maxima varies between the 800 *m* and 1200 *m* depth. The number of salinity maxima varies from one to two, sometimes three. It is interesting to see how the boundary driven main Mediterranean veins follow the poleward undercurrent by inspecting the number of salinity maxima, each maximum corresponding to one MW vein.

Figure 6 shows the ensemble average of salinity off western Iberia at 1000 *m* depth. It shows clearly the spreading extension of the Mediterranean tongue with a similar signature as that evidenced in the works of Drillet[2], Papadakis[41] and Coelho [1].

Figure 7 compares results from the Mercator solution interpolated over the *P* domain and the results from the P and C models and a NOAA satellite sea surface temperature (SST) image. All results are for the same day. Mercator results are daily average, MOHID results are instantaneous at 12h00 and the satellite image was taken during the mid-afternoon. Though it's hard to analyze the results, the MOHID finer resolution model has a higher spatial variability and is likely to resemble more the satellite SST.

#### 4 APPLICATIONS: OIL OBSERVER

One derived application of a pre-operational model simulating forecasts for hydrodynamical circulation at a regional level is an oil spill modelling system.

Oil spill models are important to support decision for operations to combat oil spills at sea. Often the positions of the slicks are monitored with the help of aircraft and thus the model is expected to make forecasts of 24-48 hours. In these situations it is important that quick answers are provided, though ensuring that the deviations that can occur within these time periods are not very large. Oil spill modelling should also be considered as an important tool to support decision makers in environmental studies and risk plans, allowing the simulation and analysis of several different pollution scenarios for hypothetical oil spills. An oil spill fate and weathering model is used in MOHID modelling system<sup>2</sup>.

By use of a lagrangian approach, MOHID is able to predict the fate and the weathering of oil spills. It simulates lagrangian tracers advected by the hydrodynamical field and by turbulent diffusion. They are characterized by properties such as density, viscosity and thickness and may endure processes such as evaporation, dispersion, emulsification, sedimentation and oil beaching. A real-case application was implemented with the MOHID system during the Prestige accident showing good agreement with remote-sensed observations[43].

---

<sup>2</sup><http://www.mohid.com>

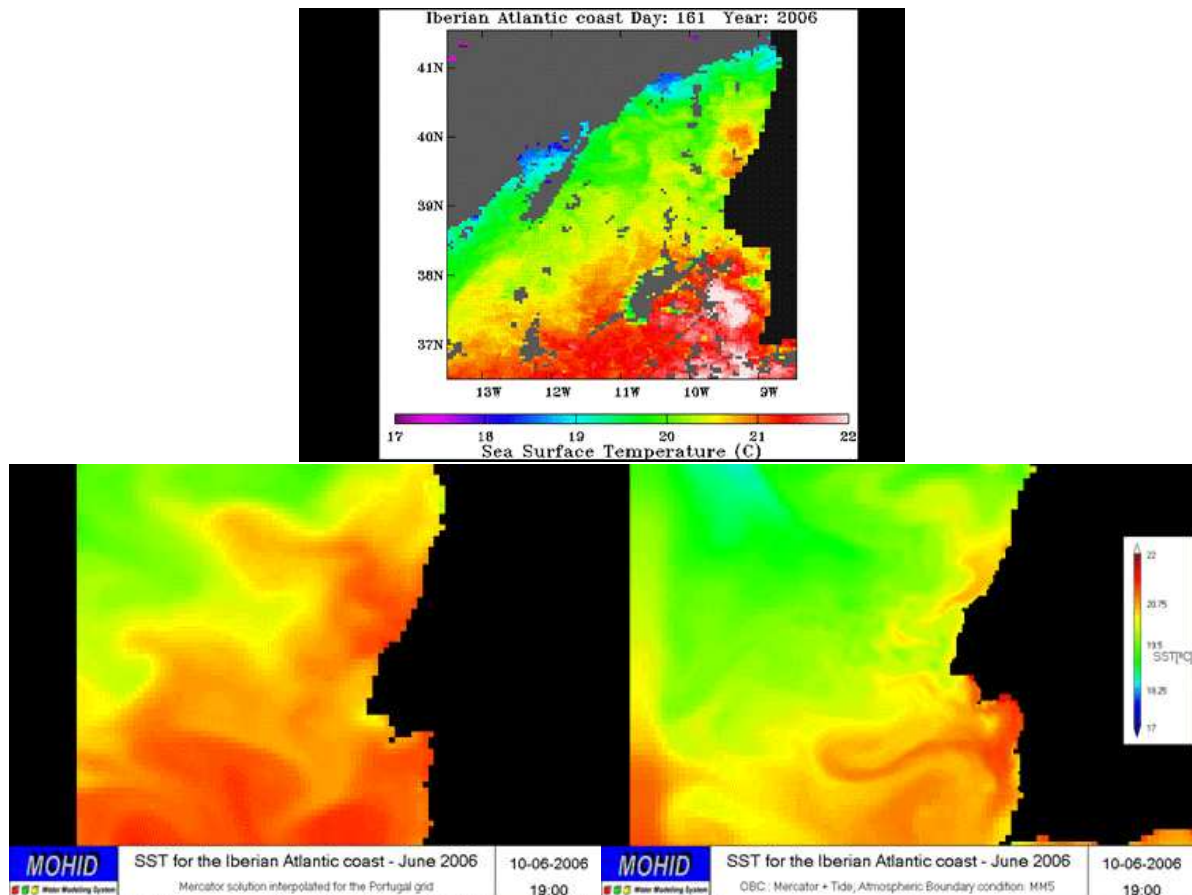


Figure 7: The Mercator solution sea surface temperature daily average on the September 9th 2006, at the bottom left. A NOAA sea surface temperature satellite image taken during the same day, at the top. At the bottom right, the Mohid instantaneous solution taken the same day at 19h00 hours. The temperature scale is set to  $[17^{\circ}C\ 22^{\circ}C]$ . However, the color palettes differs between the satellite images and the model's fields. The graphical tool used is *Mohid GIS*.

To support operations of oil spill response at sea, a web system<sup>3</sup> was developed for the Tagus area that simulates and visualizes a spill's real-time trajectory. This system (working on top of the MOHID Tagus operational model) receives input data from the end-user through a web-form. Within minutes the results are available to the end-user which can visualize them in Google Earth.

The tool may easily be ported to any other region.

## 5 CONCLUSIONS

A three-level nested tridimensional hydrodynamical model was implemented for the Portuguese coast with MOHID. It is forced with realistic ocean (Mercator, FES2004) and atmospheric (Meteo-IST) forecasts. The system is pre-operational as its results are published via an opendap server weekly since November 2006. It can provide realistic OBC to finer scale regional and local models in realtime or in offline (such as the Oil Observer). There is evidence that the finer-resolution  $E$  domain is internal-wave-permitting in contrast to its upper-scale models ( $P$  model and  $M-O$  model).

The model's MW spreading pathways scenario is realistic when compared to other works observations and analysis[30][29][2][1].

The results show a shift in the MO from a bottom current to an intermediate depth buoyancy driven current near  $8^{\circ}W$  in concordance with observations[29][30]. Also the salinity maxima observations show a realistic entrainment from the NACW in the Gulf of Cádiz.

The model's ensemble average of the salinity signature at 1000  $m$  depth occurred by non-meddy MW spreading is consistent with the works of Drillet[2] and Coelho [1].

### 5.1 Future work

Future development in this line of work towards an operational model for the Portuguese coast involves:

- To perform calculus continuations from the last reanalysis mode simulation instead of performing a one week spin-up from null velocity fields every week,
- To improve the model's outputs by calculating time series and fluxes through sections where measurements are being made,
- To assess its quality by calculating the TKE, and calculating mass balances between defined regions or boxes,
- To develop automatic satellite remote-sensing imagery acquisition and processing for comparison with the model's results.

---

<sup>3</sup><http://www.mohid.com/oilobserver>

## ACKNOWLEDGEMENTS

The authors wish to thank the Mercator-Océan team for providing the ocean forecasts and reanalysis, Meteo-IST (in particular A. R. Trancoso and J. J. Delgado Domingos) for providing the atmospheric forecasts, Thierry Lethellier for assisting in providing the FES2004 tidal atlas and the MARETEC team for the support. G. Riflet acknowledges grant SFRH/BD/17631/2004 from Fundação para a Ciência e Tecnologia.

## REFERENCES

- [1] H. S. Coelho, R. J. J. Neves, M. White, P. C. Leitão, and A. J. Santos. A model for ocean circulation on the iberian coast. *Journal of Marine Systems*, 32(1):153–179, 2002.
- [2] Y. Drillet, Bourdallé R. Badie, L. Siefridt, and C. Le Provost. Meddies in the Mercator North Atlantic and Mediterranean Sea eddy-resolving model. *Journal of Geophysical Research*, 110(C3), 2005.
- [3] F. Lyard, F. Lefevre, T. Letellier, and O. Francis. Modelling the global ocean tides: modern insights from fes2004. *Ocean Dynamics*, 56(5-6):394–415, December 2006.
- [4] R. A. Flather. A tidal model of the northwest European continental shelf. *Mem. Soc. R. Sci. Liege*, 10(6):141–164, 1976.
- [5] E. A. Martinsen and H. Engedahl. Implementation and testing of a lateral boundary scheme as an open boundary condition in a barotropic ocean model. *Coastal engineering*, 11(5-6):603–627, 1987.
- [6] J. J. Delgado Domingos and A. R. Trancoso. Meteo - ist. Internet service, 2005.
- [7] B. E. Doty, J. Wielgosz, J. Gallagher, and D. Holloway. GrADS and DODS/OPENDAP. *Proceedings of the 17th International Conference on Interactive Information and Processing Systems (IIPS) for Meteorology, Oceanography, and Hydrology*, American Meteorological Society Albuquerque, NM, 385, 2001.
- [8] K. Bryan. A numerical method for the study of the world ocean. *J. Comput. Phys*, 4:347–376, 1969.
- [9] H. Martins, A. Santos, Coelho, R. Neves, and T. Rosa. Numerical simulation of internal tides. *Proceedings of the Institution of Mechanical Engineers, Part C: Journal of Mechanical Engineering Science*, 214(6):867–872, 2000.
- [10] P. C. Chu and F. Chenwu. Finite volume ocean circulation model. *Oceans '02 MTS/IEEE*, 3:1455–1462 vol.3, 2002.

- [11] F. J. Millero and A. Poisson. International one-atmosphere equation of state of seawater. *Deep-Sea Res*, 28:625–629, 1981.
- [12] L. Umlauf and H. Burchard. Second-order turbulence closure models for geophysical boundary layers. A review of recent work. *Continental Shelf Research*, 25:725–827, 2005.
- [13] H. Burchard and Others. *Applied Turbulence Modelling in Marine Waters*. Springer, 2002.
- [14] V. M. Canuto, A. Howard, Y. Cheng, and M. S. Dubovikov. Ocean Turbulence. Part I: One-Point Closure Model Momentum and Heat Vertical Diffusivities. *Journal of Physical Oceanography*, 31(6):1413–1426, 2001.
- [15] P. D. Craig and M. L. Banner. Modeling Wave-Enhanced Turbulence in the Ocean Surface Layer. *Journal of Physical Oceanography*, 24(12):2546–2559, 1994.
- [16] A. Arakawa. Computational design for long-term numerical integration of the equations of uid motion: Two-dimensional incompressible ow. Part I. *Journal of Computational Physics*, 1(1):119–143, 1966.
- [17] F. Martins, R. J. J. Neves, and P. C. Leitão. A three-dimensional hydrodynamic model with generic vertical coordinate. *Hydroinformatics*, 98:1403–1410, 1998.
- [18] A. Beckmann and D. B. Haidvogel. Numerical simulation of flow around a tall isolated seamount. part i: Problem formulation and model accuracy. *Journal of Physical Oceanography*, 23(8):1736–1753, 1993.
- [19] A. F. Shchepetkin. A method for computing horizontal pressure-gradient force in an oceanic model with a nonaligned vertical coordinate. *J. Geophys. Res*, 108(C3):3090–3090, 2003.
- [20] N. Kliem and J. D. Pietrzak. On the pressure gradient error in sigma coordinate ocean models: A comparison with a laboratory experiment. *Journal of Geophysical Research*, 104(C12):29781–29800, 1999.
- [21] A. Adcroft, C. Hill, and J. Marshall. Representation of Topography by Shaved Cells in a Height Coordinate Ocean Model. *Monthly Weather Review*, 125(9):2293–2315, 1997.
- [22] J. J. Leendertse. *Aspects of a Computational Model for Long-period Water-wave Propagation*. Rand Corporation for the United States Air Force Project Rand, 1967.
- [23] C. A. J. Fletcher and K. Srinivas. *Computational Techniques for Fluid Dynamics 1*. Springer, 1991.

- [24] A. F. Blumberg and L. H. Kantha. Open Boundary Condition for Circulation Models. *Journal of Hydraulic Engineering*, 111(2):237–255, 1985.
- [25] N. Etopo. Bathymetry. *Product Information Catalogue*, see also <http://www.ngdc.noaa.gov/mgg/global/seltopo.html>, 1988.
- [26] E. Blayo and L. Debreu. Revisiting open boundary conditions from the point of view of characteristic variables. *Ocean Modelling*, 9:231–252, 2005.
- [27] P. Bahurel, P. De Mey, T. De Prada, E. Dombrowsky, P. Josse, C. Le Provost, P. Y. Le Traon, A. Piacentini, and L. Siefridt. MERCATOR, forecasting global ocean. *AVISO Altimetry Newsletter*, 8:14–16, 2001.
- [28] I. Ambar, N. Serra, M. J. Brogueira, G. Cabeçadas, F. Abrantes, P. Freitas, C. Gonçalves, and N. Gonzalez. Physical, chemical and sedimentological aspects of the mediterranean outflow off iberia. *Deep Sea Research Part II: Topical Studies in Oceanography*, 19(49):4137–4177, 2002.
- [29] A. S. Bower, N. Serra, and I. Ambar. Structure of the mediterranean undercurrent and mediterranean water spreading around the southwestern iberian peninsula. *Journal of Geophysical Research*, 107(C10), 2002.
- [30] M. C. Iorga and M. S. Lozier. Signatures of the Mediterranean outflow from a North Atlantic climatology 1. Salinity and density fields. *Journal of Geophysical Research*, 104(C11):25985–26010, 1999.
- [31] T. Pichevin and D. Nof. The eddy canon. *Deep-Sea Res*, 43(9):1475–1507, 1996.
- [32] T. Reynaud, P. Legrand, H. Mercier, and B. Barnier. A new analysis of hydrographic data in the Atlantic and its application to an inverse modelling study. *International WOCE Newsletter*, 32:29–31, 1998.
- [33] G. A. Grell, J. Dudhia, and D. R. Stauffer. A description of the fifth-generation Penn State/NCAR Mesoscale Model (MM5). NCAR Tech. *Note TN-398+ STR*, 122, 1995.
- [34] J. Pietrzak, J. B. Jakobson, H. Burchard, H. J. Vested, and O. Petersen. A three-dimensional hydrostatic model for coastal and ocean modelling using a generalised topography following co-ordinate system. *Ocean Modelling*, 4(2):173–205, 2002.
- [35] P. C. Leitão. *Integration of Scales and Processes in the marine Environment Modelling*. PhD thesis, Technical Superior Institute, Lisbon, 2003.
- [36] D. B. Chelton, R. A. Deszoeke, M. G. Schlax, El K. Naggar, and N. Siwertz. Geographical variability of the first baroclinic rossby radius of deformation. *Journal of Physical Oceanography*, 28(3):433–460, 1998.

- [37] D. P. Stevens. On open boundary conditions for three dimensional primitive equation ocean circulation models. *Geophysical and astrophysical fluid dynamics*, 51(1-4):103–133, 1990.
- [38] F. Auclair, S. Casitas, and P. Marsaleix. Application of an Inverse Method to Coastal Modeling. *Journal of Atmospheric and Oceanic Technology*, 17(10):1368–1391, 2000.
- [39] P. Lynch and X. Y. Huang. Initialization of the hirlam model using a digital filter. *Monthly Weather Review*, 120(6):1019–1034, June 1992.
- [40] I. Stevens, M. Hamann, J. A. Johnson, and A. F. G. Fiúza. Comparisons between a fine resolution model and observations in the iberian shelf-slope region. *Journal of Marine Systems*, 26(1):53–74, 2000.
- [41] M. P. Papadakis, E. P. Chassignet, and R. W. Hallberg. Numerical simulations of the mediterranean sea outflow: impact of the entrainment parameterization in an isopycnic coordinate ocean model. *Ocean Modelling*, 5(4):325–356, 2003.
- [42] E. Deleersnijder. Upwelling and upsloping in three-dimensional marine models. *Applied Mathematical Modelling*, 13:462–467, 1989.
- [43] C. F. Balseiro, P. Carracedo, B. Gomez, P. C. Leitão, P. Montero, L. Naranjo, E. Penabad, and V. Pérez-Munuzuri. Tracking the prestige oil spill: An operational experience in simulation at meteogalicia. *Weather*, 58:452–458, December 2003.